

Materials Horizons: From Nature to Nanomaterials

Zengbao Jiao  
Tao Yang *Editors*

# Advanced Multicomponent Alloys

From Fundamentals to Applications

 Springer

# **Materials Horizons: From Nature to Nanomaterials**

## **Series Editor**

Vijay Kumar Thakur, School of Aerospace, Transport and Manufacturing,  
Cranfield University, Cranfield, UK

Materials are an indispensable part of human civilization since the inception of life on earth. With the passage of time, innumerable new materials have been explored as well as developed and the search for new innovative materials continues briskly. Keeping in mind the immense perspectives of various classes of materials, this series aims at providing a comprehensive collection of works across the breadth of materials research at cutting-edge interface of materials science with physics, chemistry, biology and engineering.

This series covers a galaxy of materials ranging from natural materials to nanomaterials. Some of the topics include but not limited to: biological materials, biomimetic materials, ceramics, composites, coatings, functional materials, glasses, inorganic materials, inorganic-organic hybrids, metals, membranes, magnetic materials, manufacturing of materials, nanomaterials, organic materials and pigments to name a few. The series provides most timely and comprehensive information on advanced synthesis, processing, characterization, manufacturing and applications in a broad range of interdisciplinary fields in science, engineering and technology.

This series accepts both authored and edited works, including textbooks, monographs, reference works, and professional books. The books in this series will provide a deep insight into the state-of-art of Materials Horizons and serve students, academic, government and industrial scientists involved in all aspects of materials research.

### **Review Process**

The proposal for each volume is reviewed by the following:

1. Responsible (in-house) editor
2. One external subject expert
3. One of the editorial board members.

The chapters in each volume are individually reviewed single blind by expert reviewers and the volume editor.

Zengbao Jiao · Tao Yang  
Editors

# Advanced Multicomponent Alloys

From Fundamentals to Applications

 Springer

*Editors*

Zengbao Jiao  
The Hong Kong Polytechnic University  
Hong Kong, China

Tao Yang  
City University of Hong Kong  
Hong Kong, China

ISSN 2524-5384

ISSN 2524-5392 (electronic)

Materials Horizons: From Nature to Nanomaterials

ISBN 978-981-19-4742-1

ISBN 978-981-19-4743-8 (eBook)

<https://doi.org/10.1007/978-981-19-4743-8>

© The Editor(s) (if applicable) and The Author(s), under exclusive license to Springer Nature Singapore Pte Ltd. 2022

This work is subject to copyright. All rights are solely and exclusively licensed by the Publisher, whether the whole or part of the material is concerned, specifically the rights of translation, reprinting, reuse of illustrations, recitation, broadcasting, reproduction on microfilms or in any other physical way, and transmission or information storage and retrieval, electronic adaptation, computer software, or by similar or dissimilar methodology now known or hereafter developed.

The use of general descriptive names, registered names, trademarks, service marks, etc. in this publication does not imply, even in the absence of a specific statement, that such names are exempt from the relevant protective laws and regulations and therefore free for general use.

The publisher, the authors, and the editors are safe to assume that the advice and information in this book are believed to be true and accurate at the date of publication. Neither the publisher nor the authors or the editors give a warranty, expressed or implied, with respect to the material contained herein or for any errors or omissions that may have been made. The publisher remains neutral with regard to jurisdictional claims in published maps and institutional affiliations.

This Springer imprint is published by the registered company Springer Nature Singapore Pte Ltd.  
The registered company address is: 152 Beach Road, #21-01/04 Gateway East, Singapore 189721, Singapore

# Contents

## Part I High-Entropy Alloys

<b>1</b>	<b>Body-Centered Cubic High-Entropy Alloys</b> .....	<b>3</b>
	Yuan Wu, Xiaoyuan Yuan, Xiaocan Wen, and Meiyuan Jiao	
<b>2</b>	<b>Face-Centered Cubic High-Entropy Alloys</b> .....	<b>35</b>
	Weihong Liu and Boxuan Cao	
<b>3</b>	<b>Eutectic High-Entropy Alloys</b> .....	<b>53</b>
	Wenna Jiao, Zhijun Wang, Sheng Guo, and Yiping Lu	
<b>4</b>	<b>Cubic Ordered Intermetallic Alloys</b> .....	<b>91</b>
	W. C. Xiao, Y. L. Zhao, and T. Yang	

## Part II High-Temperature Superalloys

<b>5</b>	<b>Fe-Based Heat-Resistant Steels</b> .....	<b>107</b>
	Wei Yan, Shenhu Chen, Ye Liang, Yanfen Li, and Lijian Rong	
<b>6</b>	<b>Ni-Base Superalloys: Alloying and Microstructural Control</b> .....	<b>133</b>
	Shi Qiu and Zengbao Jiao	
<b>7</b>	<b>Overview of the Development of <math>L1_2</math> <math>\gamma'</math>-Strengthened Cobalt-Base Superalloys</b> .....	<b>155</b>
	Wei-Wei Xu	

## Part III Advanced High-Strength Steels

<b>8</b>	<b>Advanced High-/Medium-Mn Steels</b> .....	<b>179</b>
	Xiao Shen and Wenwen Song	
<b>9</b>	<b>G-Phase Strengthened Steels</b> .....	<b>225</b>
	Wenwen Sun and Xulong An	

<b>10</b>	<b>Intermetallic-Precipitation-Strengthened Steels .....</b>	<b>247</b>
	Mengchao Niu, Haojie Kong, Bingchen Zhou, Wei Wang, and Zengbao Jiao	
 <b>Part IV Shape Memory Alloys</b>		
<b>11</b>	<b>Abnormal Grain Growth and Single Crystals in Multicomponent Shape-Memory Alloys .....</b>	<b>269</b>
	Jixun Zhang, Tao Yang, and Shuiyuan Yang	
<b>12</b>	<b>Polycrystalline Shape-Memory Alloy and Strain Glass .....</b>	<b>287</b>
	Aleksandr Shuitcev, Yunxiang Tong, Yu Wang, and Daoyong Cong	

# **Part I**

## **High-Entropy Alloys**



# Chapter 1

## Body-Centered Cubic High-Entropy Alloys



Yuan Wu, Xiaoyuan Yuan, Xiaocan Wen, and Meiyuan Jiao

### 1 Design of BCC Refractory High-Entropy Alloys (RHEAs)

#### 1.1 Design of Single-Phase Solid Solution

It is generally accepted that the mole fraction of each constituent element in HEAs is from 5 to 35%, which greatly expands the composition range of HEAs compared to the design concept in conventional alloys. Due to the unique design concept of HEAs, some unintended second phases may form even though the high-entropy effect still exists, which may influence the related performance of HEAs. Thus, how to design single-phase HEAs with good performance is a goal pursued by materials researchers.

According to previous reports, it was found that the high mixing entropy is a pivotal factor but not an essential factor for the formation of single-phase solid solution. To improve the accuracy of prediction for designing new single-phase HEAs, the stability of single FCC or BCC HEAs can be predicted based on the atomic-size difference ( $\delta$ ) and valence electron concentration (VEC,  $\Omega$ ) as follows [1, 2]:

---

Y. Wu (✉) · X. Yuan · X. Wen · M. Jiao

State Key Laboratory for Advanced Metals and Materials, University of Science and Technology, Beijing, China

e-mail: [wuyuan@ustb.edu.cn](mailto:wuyuan@ustb.edu.cn)

© The Author(s), under exclusive license to Springer Nature Singapore Pte Ltd. 2022

Z. Jiao and T. Yang (eds.), *Advanced Multicomponent Alloys*, Materials Horizons:

From Nature to Nanomaterials, [https://doi.org/10.1007/978-981-19-4743-8\\_1](https://doi.org/10.1007/978-981-19-4743-8_1)

$$\begin{aligned}
\delta &= \sqrt{\sum_{i=1}^N c_i (1 - r_i/\bar{r})^2} \\
\bar{r} &= \sum_{i=1}^n c_i r_i \\
\Omega &= \sum_{i=1}^n c_i \Omega_i
\end{aligned} \tag{1}$$

where  $c_i$ ,  $r_i$ , and  $\Omega_i$  are atomic percentage, atomic radius, and VEC of the  $i$ th component, respectively. Combined with  $\delta$  and  $\Omega$  according to the abundant experimental data [3, 4], the single-phase solid solution can be formed when  $\Omega > 1.1$  and  $\delta < 6.6\%$ . FCC phase is stable when  $\text{VEC} > 8$  and BCC phase is stable when  $\text{VEC} < 6.87$ . In spite of the fact that these parameters are based on statistical experimental data, it is significant and instructive for designing novel single-phase HEAs. Moreover, researchers propose the thermodynamic criterion combined with the inherent physical and chemical properties of the constituent elements, such as Gibbs free energy [5], mixing enthalpy and entropy [6], and vacancy exchange potential [7], which can further improve the accuracy of the prediction for designing single-phase HEAs combined with the empirical equation.

The development of new high-performance materials is getting faster and faster. Conventional single-phase solid solution cannot meet the demand for high performance under different conditions, especially the harsh environments. Thus, the development of novel high-performance HEAs is not limited to single-phase structures. Because the BCC HEAs mainly consist of refractory elements, we will focus on the performance-oriented composition design of the refractory HEAs (RHEAs) in the next parts.

## 1.2 Development of RHEAs with Good Wear Resistance

Due to the high solid-solution strengthening effect which is the intrinsic property of HEAs, the wear resistance in HEAs is inevitably better than that in conventional alloys, such as Ni-based superalloys and SS304 stainless steel [8–11], as shown in Fig. 1. The increment of the wear resistance can be dominated by the wear film formed on the surface, which is related to the oxides combined with the constituent elements. For example, some easily oxidized elements, such as Ti and Zr, can form oxide film more easily on the surface [9], which can improve the wear resistance resulting from the lubrication effect of the film. Thus, the component design for improving wear resistance should consider some elements which can form oxides [9, 11], or silicides [12] with a continuous and dense structure under corresponding friction conditions. Moreover, the temperature is another key factor to the wear resistance. Different

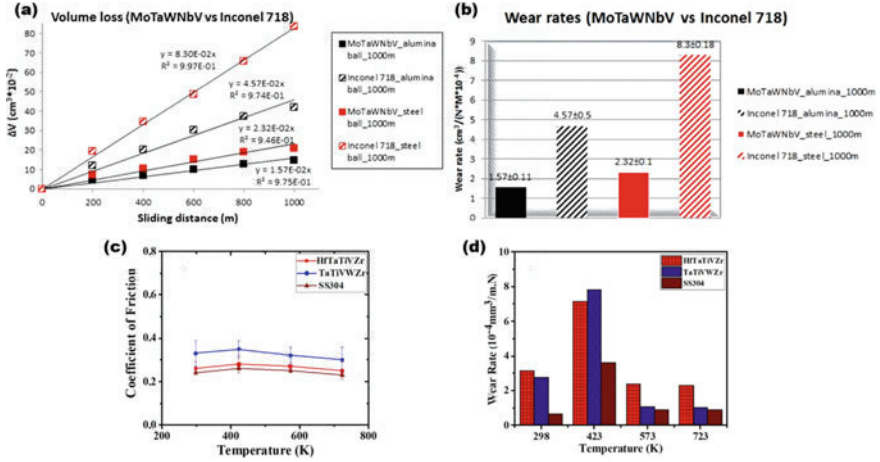


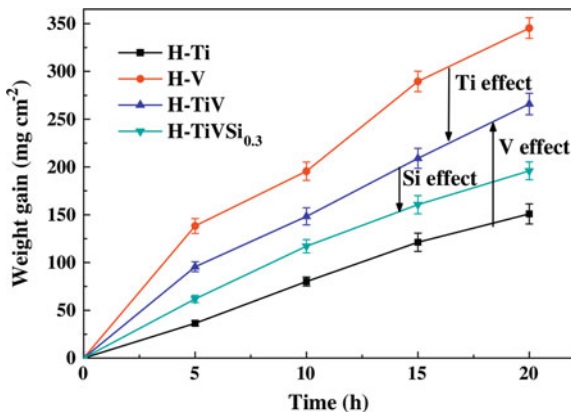
**Fig. 1** **a** and **b** are the comparison of the volume loss as a function of the sliding distance and the wear rates for  $\text{Mo}_{20}\text{Ta}_{20}\text{W}_{20}\text{Nb}_{20}\text{V}_{20}$  and Inconel 718, respectively [10]. **c** and **d** are the steady-state coefficient of friction and wear rate for HfTaTiVZr, TaTiVWZr, and SS304 as a function of temperature, respectively [11]

films exhibit different characteristics under different temperatures.  $\text{Al}_2\text{O}_3$  film is still continuous and dense at elevated temperatures, while the nitride film becomes incompact [13]. The silicide film has a good wear resistance from ambient to intermediate temperatures, but its wear properties are not clear at high temperatures [12]. Thus, the component design for the wear resistance should consider the application temperature. Yet, there are slight researches on friction and wear properties for RHEAs, especially for their tribological behavior at the elevated temperatures. More investigations are needed for the guidance to develop novel wear-resistance RHEAs.

### 1.3 Development of RHEAs with Good Oxidation Resistance

The service temperature of conventional Ni-based superalloys is higher than 1100 °C, which has approached the ultimate service temperature of the metal material. Such service conditions impose some special peculiarities on the material, i.e., excellent high-temperature stability, strength, and oxidation resistance. Compared to the Ni-based superalloys, generally, the constituent elements in BCC RHEAs are the refractory elements, such as Nb, Mo, and Ta, which make the BCC RHEAs withstand higher temperatures without melting [13]. Besides, the BCC RHEAs have higher high-temperature stability, strength, and softening resistance compared to the conventional superalloys in the previous research [14]. Thus, good oxidation resistance is inevitable and necessary for the BCC RHEAs applying and working in the high-temperature environment.

**Fig. 2** Isothermal oxidation curves for the HEAs at 1300 °C, showing the effects of Ti, V, and Si addition [15]



Outstanding oxidation resistance is dominated by the oxide film formed on the metal surface with stable chemical properties, denseness, good combination with matrix, and fewer defects during the oxidation process to hinder the further oxidation of the alloy and protect the matrix. But according to the characteristics of the primary refractory metal elements in the BCC RHEAs, such as Nb, Mo, Ta and W, the oxidation resistance of these refractory elements under high temperature is unsatisfactory. To improve the oxidation resistance of BCC RHEAs, the oxidation-resistant film constituted with the component elements must have a good antioxidant capacity. Thus, some alloy elements, such as metallic elements Al and Cr, and non-metal element Si, are added to the BCC RHEAs [15–19]. For example, Ti, V, and Si were added, and the content of these elements was adjusted in the NbCrMoAl<sub>0.5</sub> RHEA [15], as shown in Fig. 2. The results show that the compact Al<sub>2</sub>O<sub>3</sub> film was generated due to Al in the matrix, and the addition of Ti and Si can also produce compact (TiCrNb)<sub>2</sub>O<sub>3</sub> film at 1300 °C. Both the two films were dense, and the oxidation resistance in this RHEA was improved significantly. However, porous VO<sub>x</sub> film with a low melting point [13] was formed and further deteriorated the oxidation resistance. Therefore, from the viewpoint of alloy design, we should consider not only whether the film is dense but also the melting point of the formed oxide film under high temperatures. Until now, Ti, Cr, Si, and Al are preferred to be added to the BCC RHEAs to improve the oxidation resistance on one hand and lower the density on the other hand.

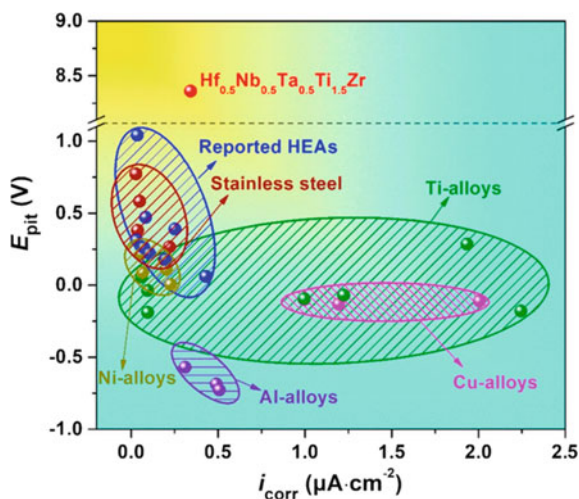
#### 1.4 Development of RHEAs with Good Corrosion Resistance

Similar to the wear and oxidation resistance mechanism in BCC HEAs, the corrosion resistance of alloys is also related to the film formed on the surface in different solutions. The film usually is a passivation layer which can reduce the reaction rate with the surrounding solution and further protect the matrix from corrosion [20].

From the previous research about the corrosion resistance of BCC RHEAs, the BCC RHEAs have a more excellent corrosion resistance in the high concentration of sulfuric acid, hydrochloric acid, nitric acid, etc. compared to conventional stainless steels, Ti-alloys and Cu-alloys [21, 22], as shown in Fig. 3. This phenomenon is mainly due to the fact that the elements used in conventional alloys to improve the corrosion resistance, such as Ta, Mo, Al, and Cr, have become the primary constituent elements in BCC RHEAs [20]. Besides, due to the unique characteristics of high entropy, the BCC RHEAs have some superiorities compared to the conventional alloys [23]. First, the high-entropy effect improves the forming ability of single phase, which can reduce the possibility of element segregation and thus can promote a uniform film formed on the surface to improve the passivation ability and pitting resistance. Second, the sluggish diffusion effect lowers the diffusion rate of the element from the matrix to surface, which can retard the alloy elements diffusing to the surface when the alloy is corroded. As a result, the corrosion and cauterization of the RHEAs are delayed. Last, the lattice distortion effect may impede the movement of the atoms, which may improve the stress corrosion. Therefore, the BCC RHEAs have enormous potential as corrosion-resistant materials.

The BCC HEAs usually consist of elements which can form a passivation film. But different passivation films formed by different elements existing different characteristics in different solutions. For example, Zhang et al. studied the corrosion resistance of the base alloy  $\text{TiZr}_{0.5}\text{Nb}$  containing Cr, V, and Mo [24]. The result shows that all the alloys exhibit excellent corrosion resistance in the NaCl and  $\text{H}_2\text{SO}_4$  solutions. Among the three alloys, V and Mo decrease the resistance to general corrosion and increase the pitting corrosion resistance for the series of alloys in the NaCl solution slightly, while they greatly improve the corrosion resistance in the  $\text{H}_2\text{SO}_4$  solution.  $\text{TaNbHfZrTi}$  can generate a  $\text{Ta}_2\text{O}_5$  passivation film, which is very stable in the  $\text{HNO}_3$  environment [24]. However, in fluorine ions containing  $\text{HNO}_3$  solution, the corrosion

**Fig. 3** Comparison of pitting potential and corrosion current density for the  $\text{Hf}_{0.5}\text{Nb}_{0.5}\text{Ta}_{0.5}\text{Ti}_{1.5}\text{Zr}$  RHEA, previously reported HEAs, and some conventional passive alloys in the 3.5 wt% NaCl solution [22]



rate is much higher compared with the alloy in the  $\text{HNO}_3$  solution. The reason is that the Zr and Hf can form fluoride with fluorine ions more readily. By the way, the corrosion resistance of  $\text{Ti}_{1.5}\text{ZrHf}_{0.5}\text{Nb}_{0.5}\text{Ta}_{0.5}$  RHEA is much better than that of 316L stainless steel in the NaCl solution due to the high pitting potential [22]. Thus, the alloy design for the corrosion resistance should consider the chemical reaction between the constituent elements and the solution environment and lower the content of the disadvantageous element. Now, recent researchers come to notice that not only the chemical component but also the special structure and physical characteristics lead to the excellent corrosion resistance of BCC RHEAs [20], and it is expected to evolve RHEAs with better corrosion resistance than the existing alloys in the future.

### ***1.5 Development of RHEAs with Good Mechanical Properties***

To obtain better mechanical properties no matter at ambient temperature or high temperatures, the single-phase BCC RHEAs are not limited to investigations from scholars nowadays. The abundant composition variability of BCC RHEAs provides plenty of opportunities to process and generate the desired phase structure to control the property of ultimate alloys. However, that will lead to a predicament, i.e., how to choose an appropriate chemical constituent from a mass of possible constituents. Different from chemical compositions, accurately grasping the commonness and characteristics of elements and determining the relationship between the structure and properties of the alloys can better and more accurately guide the design and optimization of BCC RHEAs, which will greatly reduce the amount of trial and error experiments.

The component elements in BCC RHEAs can be classified into BCC stabilizer elements (W, Mo, Nb, Ta, and V), HCP stabilizer elements (Hf, Zr, and Ti), high mixing entropy elements (Cr, Co, and Al), and non-metallic elements (C, N, O, B, Si, etc.) according to their features. The stabilizer elements are conducive to forming a single BCC structure, which can improve the phase stability of the alloy significantly at high temperatures [14]. At ambient temperature, the stabilizer elements also can inhibit the formation of second phases and enhance the mechanical properties. The primary mechanical properties of RHEAs are focused on the compression properties [25–27]. The RHEAs with good tensile properties usually are the series of  $\text{TiZrHfNbTa}$  HEAs [28–30]. The TRIP effect was introduced into a  $\text{TiZrHfTa}$  RHEA via regulating the concentration of the BCC stabilizer element Ta [29], resulting in a good combination of high strength and plasticity due to the transformation of the metastable BCC phase during tension. The HCP stabilizer elements have an HCP structure at low temperatures and BCC structure at high temperatures [31, 32]. The inclusion of these elements in the BCC HEAs is beneficial to promoting the equilibrium of strength and toughness of the alloys and improving the plasticity of the alloys at the same time [33]. Besides, taking advantage of the instability of HCP

elements at the intermediate temperatures in the BCC RHEAs, the size and distribution of the precipitates enriched with HCP elements can be controlled by appropriate heat treatment processes, and the mechanical properties can be improved [34]. The elements with high mixing entropy have negative mixing enthalpy with most refractory elements, resulting in a strong interaction during alloying. High mixing enthalpy can easily destroy the formation of single-phase disordered solid solution during solidification and promote the formation of new intermetallic compounds or lead to the formation of ordered phases. The BCC RHEAs containing Cr will form Laves phase when solidification [35–37], and the second phase has a significant reinforcement effect, showing excellent strength but low plasticity at the ambient temperature. Only a single-phase structure containing Al can improve the strength and plasticity of the alloys [38–40]. Increasing the Al content promotes the formation of ordered phases, such as the B2 phase, which makes the strength and plasticity decrease [41]. By the way, the high mixing entropy elements usually have a lower density than that of the primary constituent elements and thus reduce the density of the BCC HEAs on the one hand, and can improve the high-temperature oxidation resistance on the other hand, which plays an important role for high-temperature applications. The non-metallic elements added to the BCC HEAs can be classified into two types, i.e., Si with a large atom size which can form the silicide with the refractory elements readily, and B, C, N, O with a small atom size which usually occupy the interstitial lattice site. With the increase of Si additions in the NbMoTaW RHEA, the yield strength increases while the plasticity decreases. The appearance and increase of the silicide phase have a strong constraint on the matrix and hinder the motion of the dislocations, thus improving the strength of the alloy [12]. Lei et al. added 2% (atomic fraction) of oxygen to the TiZrHfNb BCC RHEA to generate the ordered oxygen complexes (OOCs) [30], as shown in Fig. 4. The OOCs act on the dislocations and cause the dislocation pinning, making the plastic flow more uniform. The addition of carbon in a TiZrHf<sub>0.5</sub>NbMo<sub>0.5</sub> RHEA improves the fracture strength and plasticity at ambient temperature, which results from the decrease of the solid-solution strengthening [42]. In general, the non-metallic atoms with a small size lead to the lattice distortion in alloys to hinder the dislocation motion, thus obviously playing a role in strong toughness.

The RHEA is considered to be the most promising alloy in the next-generation superalloys. However, the cost of preparing RHEAs is high, and the scholars hope to improve the high-temperature performance via precipitation strengthening, which is similar to the Ni-based superalloys. Laves phase is an important reinforced phase in conventional alloys. The formation of Laves phase is mainly related to Cr, Mo, and Zr, which are beneficial to improve high-temperature properties [35, 37, 43, 44]. Thus, the Laves phase can be easily obtained in RHEAs, which can significantly improve the high-temperature oxidation resistance and mechanical properties. Another high-temperature reinforcement phase is the ordered B2 phase [45, 46]. The B2 phase can exist in the matrix of as-cast alloys or in the alloys after annealing at 1200 °C, and the common elements in these alloys are Al, Ti, Zr, and Nb [47, 48]. Meanwhile, Senkov found that the B2 phase can be formed by the decomposition of high-temperature BCC phase [45]. The coherent precipitation of the disordered plate-like BCC particles



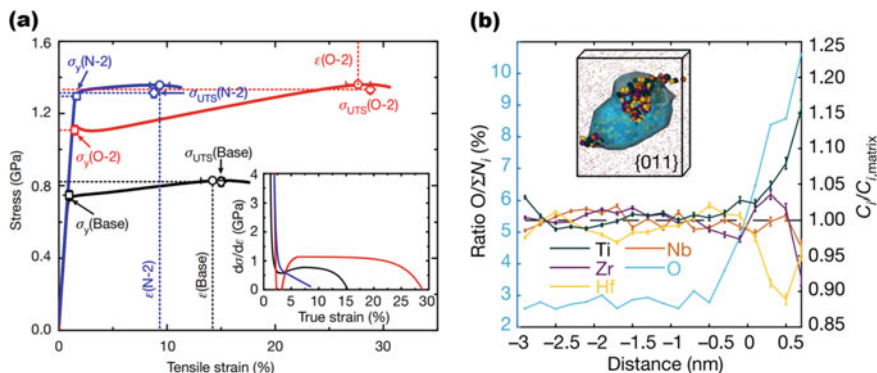


**Fig. 4** **a** Room-temperature tensile stress–strain curves for the as-cast TiZrHfNb, (TiZrHfNb)<sub>98</sub>O<sub>2</sub> and (TiZrHfNb)<sub>98</sub>N<sub>2</sub> HEAs. **b** O composition profile as a function of the distance to the interface for a selection of particles (left axis) and evolution of the composition of the main constituents relative to their respective matrix composition (right axis) [30]

forms on the ordered B2 matrix, which is similar to the coherent precipitation of L1<sub>2</sub> in the FCC matrix in Ni-based superalloys, resulting in excellent high-temperature oxidation resistance and strength.

## 1.6 Development of RHEAs with Good Irradiation Resistance

The first report about the irradiation resistance in HEA was in 2012 [49]. The researchers developed a novel equimolar ZrHfNb alloy with a single BCC phase according to which the elements are frequently used for nuclear materials. Several irradiation-resistant HEAs have been reported over the past decade, including FCC HEAs, such as FeCoNiCrCu [50] and FeNiCrMn [51], and BCC HEAs, such as Ti<sub>2</sub>ZrHfV<sub>0.5</sub>Mo<sub>0.2</sub> [52] and W<sub>38</sub>Ta<sub>36</sub>Cr<sub>15</sub>V<sub>11</sub> [53]. It is found that the HEAs had a more excellent irradiation resistance than the conventional irradiation-resistant alloys, such as stainless steels whether under the electron, helium ion, and neutron irradiation, as shown in Fig. 5. It may make the HEAs the potential radiation-resistant material.

In BCC RHEAs, the mechanism of irradiation resistance originates from the high entropy. The high-entropy effect brings a unique structure and physical characterizations in the irradiation-resistant BCC RHEAs. In contrast to conventional alloy systems, the high entropy of mixing effect tends to stabilize the single solid-solution structure, which makes the RHEAs a low activation property under irradiation [54]. The severe lattice distortion in RHEAs makes the overlap region between the migration energy of vacancies and interstitials broad, which is beneficial in delaying the irradiation-induced dislocation loop growth [55, 56]. The sluggish diffusion effect may hinder the migration of the atoms and thus delay the irradiation damage [57].



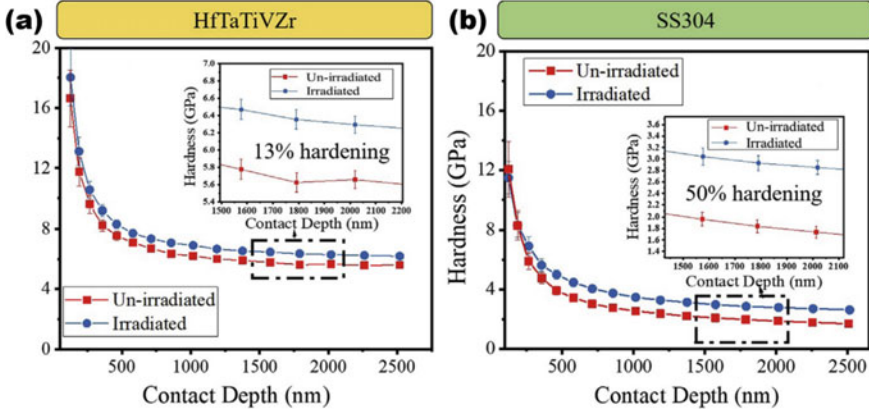


**Fig. 5** Hardness versus depth for irradiated and un-irradiated samples of **a** HfTaTiVZr HEA and **b** 304 stainless steels [54]

Another radiation-resistant mechanism in RHEAs may come from the “self-healing” process [58, 59]. RHEAs containing several primary elements have different local chemical environment [60], and thus many types of atomic vacancies and interstitials form under irradiation, exhibiting extremely high formation energy and high atomic-level stress as well as low migration energy [59]. These unstable vacancies and interstitials promote amorphization and follow by recrystallization. Due to the fact that Ti, Zr, and Hf are usually added to the RHEAs which is common in amorphous, it is easy for the cyclic process between amorphization and recrystallization, resulting in the high recombination rate for the annihilation of the defects and thus improving the irradiation resistance.

Until now, however, the effect of different elements on the irradiation resistance as well as the mechanical properties before and after irradiation in RHEAs is less studied. More investigations need to be conducted, and the development of novel RHEAs with good irradiation resistance is a long way to go.

## 2 Microstructures of BCC RHEAs

### 2.1 Single-Phase Solid Solution

The crystal structure is one of the basic factors that determine the physical, chemical, and mechanical properties of solid metals. Studies on RHEAs have found that the high mixing entropy enhances the phase stability of the solid solution, which hinders the formation of intermetallic compounds and promotes the formation of simple solid solutions in the alloys, a phenomenon that is more pronounced at high temperatures.

One of the most famous BCC RHEAs is the Senkov alloy [61], which contains Nb (BCC), Mo (BCC), Ta (BCC), and W (BCC) in equal molar ratios, and the as-cast sample has a single-phase BCC crystal structure, showing typical dendritic features. The quaternary alloys were then expanded to quintuple alloys by adding V (BCC) or Ti (HCP), and the as-cast alloys with different lattice parameters exhibited simple BCC solid-solution structures [62]. These two alloys exhibit outstanding softening resistance and thermal stability at ultra-high temperatures, but suffer from room-temperature brittleness, which severely limits their processability and thus practical applications. In addition, Al acts as a strong BCC stabilizer [63–65] and tends to form strong bonds with the constituent elements within specific RHEA systems, such as TiZrNbHfTa. Thus, Al additions to TiZrNbHfTa are expected to improve the oxidation resistance, high temperature strength, and maintain a BCC solid-solution structure [63].

Due to the inherent properties of BCC RHEAs and the large atomic-radius difference between the interstitial atoms and basic elements of HEAs, interstitial C, N, or O atoms can also play a huge role in the crystal structure of alloys. In particular, there are some interesting research results. Recently, Wang et al. [66] successfully achieved a large plasticity of >10%, along with a high strength of >1750 MPa in the NbMoTaW RHEAs via grain boundary engineering with the addition of either metalloid B or C. Microalloying of B or C atoms which preferentially segregate to grain boundaries suppresses the O segregation at grain boundaries. A strong electronic interaction between B/C and the host metals ensures a strong bonding to adjacent metallic atoms, which contributes to the enhanced cohesion. Meanwhile, the enhanced grain boundary cohesion successfully suppressed the early intergranular crack and changed the deformation mode from intergranular to intragranular, eventually contributing to the plasticity enhancement. Moreover, the boron doping induced a high efficiency in grain refinement from 96.0 to 16.2  $\mu\text{m}$  of the TiZrNb MEA, which is the main factor for strengthening. Dislocation-dominated deformation mechanism involving cross-slip and dislocation pining in the TiZrNb containing 500 ppm boron serves to enhance the strain-hardening capacity, leading to the enhancement of ductility [67].

It has been empirically established that the competition between the configuration entropy and enthalpy, the difference between the atomic radius and electronegativity of constituent elements [31, 41], and also the overall valence electron concentration [2] are a few key thermodynamic parameters for the formation of HEAs. All these parameters are very susceptible to pressure tuning. Actually, pressure is a very powerful tool to tune the atomic/electronic structure of various materials and has been employed to understand materials and search for novel materials through rich pressure-induced phase transitions in diverse systems. Therefore, in contrast to the seeming ultra-stability during heating or cooling, BCC HEAs might exhibit rich tunable behavior under high pressures. Ahmad et al. investigated the structural stability of a TiZrHfNb alloy with a disordered BCC structure during compression up to 50.8 GPa, and no phase transition was found [68]. Yusenko et al. explored another BCC-structured  $\text{Al}_2\text{CoCrFeNi}$  HEA which transitioned up to 60 GPa, and no phase was found as well [69]. Moreover, the structural evolution of a  $(\text{TaNb})_{0.67}(\text{HfZrTi})_{0.33}$  HEA during compression up to  $\sim 100$  GPa seemed very

robust without any detectable structural transition [70]. No phase transition was ever observed in the BCC-structured HEAs. Therefore, it seems that the BCC-structured HEAs are incredibly stable, and much higher pressure may be needed to induce phase transition. To lower the transition pressure of possible polymorphic phase transitions, Cheng et al. [71] chose an equiatomic AlCoCrFeNi HEA and monitored its structural evolution during compression up to 42 GPa. The AlCoCrFeNi alloy had an ordered BCC structure (B2 phase) and was reported to sit in the transition zone between the FCC and BCC phases, as  $x$  varies in the  $\text{Al}_x\text{CoCrFeNi}$  HEA system ( $0 < x < 2$ ) [72]. Indeed, they discovered a phase transition from the initial B2 phase to a highly distorted form starting at relatively low pressure of  $\sim 17.6$  GPa. Besides the XRD peak splitting, severe peak weakening and broadening occurred during compression, which may have been caused by the significant lattice distortion developed in the sample. Therefore, their work was unable to resolve the atomic structure of the high-pressure phase. Nevertheless, it is the first time that a pressure-induced polymorphism was suggested in a BCC-structured HEA [71].

## 2.2 Short-Range Orderings (SROs)

Recently, a large number of studies reveal that the arrangement of atoms in HEAs is not an ideal disordered state due to the diversity in atomic radii and the complex interactions between the constituent elements usually result in SRO structures during solidification or/and heat treatment processes [73–77]. Furthermore, the SROs observed in HEAs affect the mechanical and physical properties of alloys. It seems that the existence of topological and/or chemical SROs is one of the common yet key features of HEAs, and the manipulation of SROs may provide an effective way for tuning the properties of HEAs. In fact, SROs have been widely reported in different types of BCC RHEAs. For instance, Bu et al. [77] studied the local chemical fluctuation in a HfNbTiZr HEA and employed in situ TEM straining to investigate the deformation behaviors of the ductile BCC HfNbTiZr HEA. It was demonstrated that local chemical fluctuations (LCFs) induced dislocation pinning (Fig. 6), multiplications and cross-slips in the HfNbTiZr HEA. The pinning caused by the LCFs not only increases the dislocation motion barrier, but also stimulates dislocation multiplication. The local double cross-slips make the dislocations multiplication occur onto various planes, which effectively alleviates strain localization. Furthermore, Lei et al. [30] reported that the addition of 2% oxygen in the TiZrHfNb HEA promotes the formation of the OOCs since oxygen prefers to stay with the Ti/Zr atoms, as clearly shown in Fig. 7. The unique SROs of interstitial solutions play a decisive role in the mechanical properties. The SROs in  $(\text{TiZrHfNb})_{98}\text{O}_2$  HEA act as precipitates to interact with dislocations by pinning and facilitate frequent dislocation cross-slip, leading to the change of the plastic deformation mode from planar slip to wavy slip.

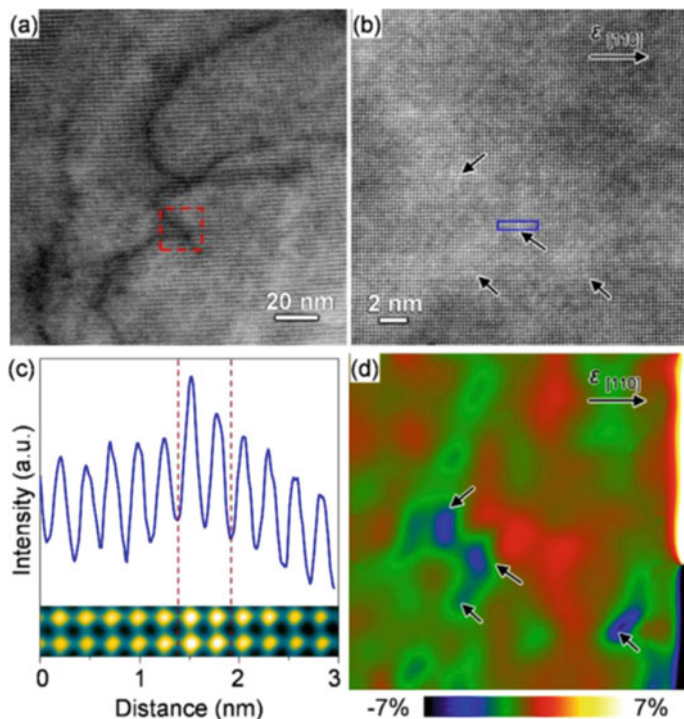


**Fig. 6** LCF-induced pinning. **a** A low-magnification bright field (BF)-scanning transmission electron microscopy (STEM) image of a pinned dislocation. **b** The high-resolution HAADF-STEM image corresponding to the square area in (a). **c** Intensity line profiles of the blue squared region in (b), inset is the corresponding enlarged HAADF-STEM image. **d** The geometric phase analysis (GPA) of (b) shows the strain fluctuation around the pinning point [78]

### 2.3 Intermediate and Complex Phases

It was found that there are many factors affecting the formation of RHEAs [79], including mixing entropy, mixing enthalpy, atomic-size difference, and valence electron concentration. When the enthalpy of formation of intermetallic compounds is large enough to overcome the effect brought about by the high-entropy effect, intermediate or complex phases are generated.

The HCP phase only appears as a second phase in some RHEAs containing Hf, Ti, and Zr. As a strong BCC stabilizer, Ta and Nb play an important role in phase formation in these HEAs [29, 80]. Huang et al. [29] used the TaHfZrTi high-entropy alloy as a model material and successfully designed the Ta<sub>x</sub>HfZrTi two-phase RHEA with excellent mechanical properties by regulating the thermodynamic and mechanical stability of the phases. As shown in Fig. 8 [29], the transformation-induced plasticity (TRIP) effect induces the formation of the HCP phase, which exists as a second phase. Phase transformation yields an intensive strain-hardening effect by dynamic

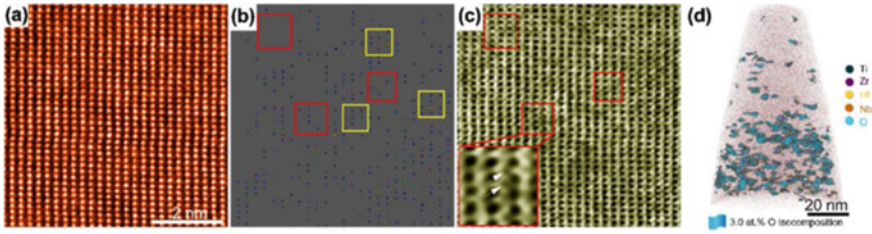


**Fig. 7** Chemical characterizations of ordered oxygen complexes (OOCs) in the  $(\text{TiZrHfNb})_{98}\text{O}_2$  HEA. **a** The HAADF-STEM image for the  $[011]$  BCC crystal axis with a differently adjusted contrast to reveal the existence of chemical short-range ordering. **b** The atomic number contrast analysis of the HAADF-STEM image reveals the OOCs. Red squares represent the Zr/Ti-rich regions, and yellow squares indicate the Hf/Nb-rich regions. **c** The aberration-corrected STEM-annular bright field image. The inset in (c) is an enlarged view of the OOCs, with the white arrows indicating the positions of the oxygen atom columns. **d** APT reconstruction of the O-doped HEA [30]

strain–stress partitioning between the BCC and HCP phases and promotes plastic deformation inside grains, which effectively suppresses early cracking and eventually gives rise to an outstanding combination of strength and ductility. Similarly, with the increase of Nb content in  $\text{HfNb}_x\text{Ta}_{0.2}\text{TiZr}$  ( $x = 0, 0.15, 0.20$  and  $0.25$ ) HEAs, phase constitution exhibits a transition from a nearly single HCP phase (i.e., Nb0) to dual phases of BCC and HCP, i.e., Nb0.15 and Nb0.2 [80]. It was found that proper addition of Nb could not only enhance the TRIP effect due to the reduced phase stability of the prior BCC phase, but also facilitate twinning in the product HCP (hexagonal close packing) phase at the late stage of deformation [80]. Moreover, Stepanov et al. [36] investigated the organization and hardness of  $\text{HfNbTaTiZr}$  alloy after annealing treatment.  $\text{HfNbTaTiZr}$  alloy precipitated nanoscale HCP phase in BCC matrix after annealing at 600 and 800 °C. The nanoscale HCP phase particles are distributed in the grain boundaries, which substantially increase the hardness of the alloy.

Some of the RHEAs have a two-phase microstructure containing either two BCC phases, BCC and B2, or BCC and Laves phases [81]. Reports on the formation of B2 structure of RHEAs which contain Al, Ti, Nb, and Zr. The B2 phase can be present as a matrix phase in as-cast or 1473 K annealed HEAs [45, 46, 82]. Interestingly, most of the Al-containing RHEAs have a superalloy-like two-phase microstructure containing BCC and B2 phases [47, 83–86]. And the disordered BCC phase is usually present in the form of cuboidal nanoscale precipitates arranged along  $\langle 100 \rangle$  directions in a coherent B2 matrix. Jensen et al. [87] studied the  $\text{AlMo}_{0.5}\text{NbTa}_{0.5}\text{TiZr}$  RHEA that the arrangement of BCC cuboidal nanoprecipitates is along  $\langle 100 \rangle$  directions with thin continuous B2 channels around them. This alloy shows a compressive yield strength of  $\sim 750$  MPa at 1000 °C, which exceeds the capability of any superalloys. While the ductility is very low at room temperature, which is attributed to the continuous ordered B2 matrix of this alloy [83]. Wang et al. [41] found that Al addition in the HEAs results in a notable strengthening effect, which is attributed

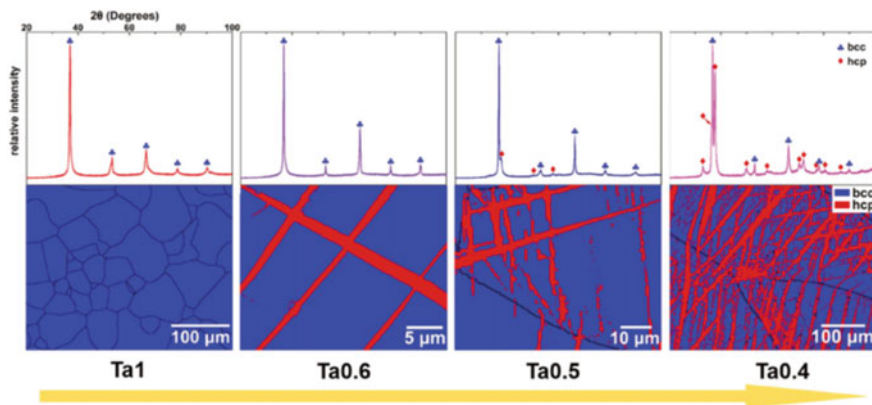


**Fig. 8** XRD patterns and EBSD images of the as-cast  $Ta_x$  HEAs. The Ta concentration significantly influences the phase constitution of this alloy system, rendering either single (BCC) or dual-phase (BCC + HCP) structure. The decreasing of Ta content destabilizes the BCC matrix and promotes formation of HCP [29]

to solid-solution hardening and ordered phase hardening. When the amount of Al exceeds the solubility in a random solid solution, an ordered BCC phase with the lattice constant close to random one starts to form. The high electron density and Fermi level of Al contribute to the formation of covalent bonds. VEC and  $\Omega$ - $\delta$  criteria seem to more precisely predict the formation of solid solutions. A low VEC value may be in favor of ordering structural transition of BCC phase [41].

Laves phase, which is related to Cr, Mo, and Zr, is an important strengthening phase in conventional alloys, leading to excellent high-temperature properties. It was found that introducing the Laves phase into refractory high-entropy alloys can significantly improve the oxidation resistance [43, 44], creep resistance, and mechanical properties [35–37], while inevitably reducing the room-temperature plasticity. Considering the low density of Cr and the high solubility with refractory elements [88], it can be used to reduce the density of HEAs and the Laves phase is present in the alloy in the form of large particles or fine precipitates. It was found that Al can be used as an alternative to Cr to prepare RHEAs resistant to high-temperature oxidation [18], which can not only reduce the density of the alloy, but also improve the strength.

### 3 Mechanical Properties of BCC HEAs

In recent years, the emergence of HEAs, which is consisting of multiple principal elements in equimolar or near-equimolar ratios, has attracted extensive attention due to their unique phase constitution, structure characteristic, and outstanding mechanical behavior, such as high hardness, strength, and fracture toughness [89, 90].



Overall, it has been reported that BCC-structured HEAs show higher strength and lower plasticity compared with FCC-structured HEAs, which indicates that the structure types are the dominant factor in controlling the strength or hardness of HEAs. In this section, we review some of the BCC HEAs concerning mechanical properties.

### 3.1 Mechanical Behavior at Room Temperature

The room-temperature mechanical properties of BCC HEAs can be varied over a wide range depending on the phase constitution, heating treatment processing, and loading method (i.e., tensile or compression).

The BCC-structured HEAs typically exhibit high strengths although the plasticity is poor. Therefore, the present reported mechanical property is mostly focused on compression tests. For instance, Senkov et al. [14] conducted the room-temperature compressive test of the NbMoTaW and VNbMoTaW HEAs (Fig. 9), where the yield strengths were 1058 and 1246 MPa, respectively, while the elongation was 1.5% and 1.7%, respectively. Limited compressive plasticity at room temperature suggests that the ductile-to-brittle transition for these alloys occurs above room temperature. After compression deformation, scanning electron microscopy imaging revealed that the fracture morphologies of the alloys contained a brittle quasi-cleavage fracture, suggesting that in this alloy, the primary failure mode is tensile rather than shear.

The TaNbHfZrTi RHEA has been observed to exhibit relatively high strength and good plasticity [91]. For instance, it was found that this alloy exhibited a yield strength approaching 929 MPa, and a compression plasticity surpassing 50% at room temperature (Fig. 10). The excellent comprehensive mechanical properties were attributed to the synergy of solid-solution strengthening effect, dislocation slip, and twinning.

Wang et al. [66] recently reported that doping small-sized metalloids boron or carbon in NbMoTaW RHEAs could preferentially replace oxygen at grain boundaries and promote stronger electronic interaction with the host metals, thus effectively

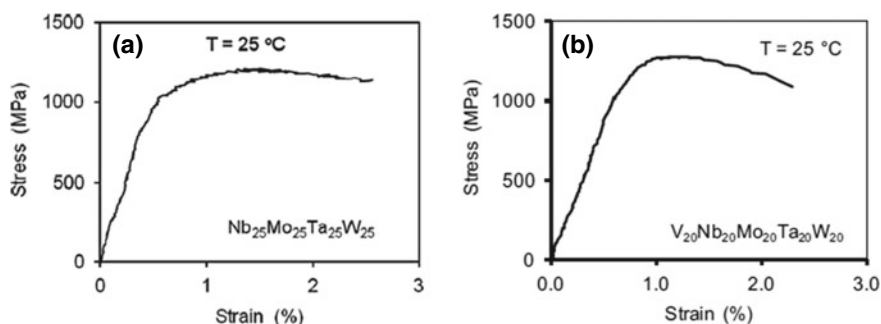
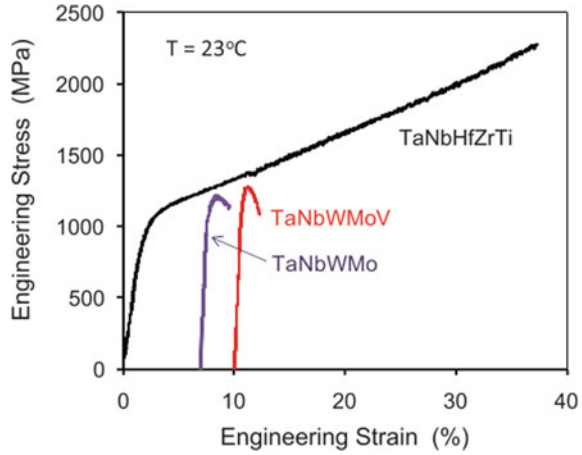


**Fig. 9** Compressive engineering stress–strain curve of the NbMoTaW and VNbMoTaW HEA at room temperature [14]

**Fig. 10** Engineering stress versus engineering strain compression curves of the  $\text{Ta}_{20}\text{Nb}_{20}\text{Hf}_{20}\text{Zr}_{20}\text{Ti}_{20}$  alloy and  $\text{Ta}_{20}\text{Nb}_{20}\text{W}_{20}\text{Mo}_{20}\text{V}_{20}$  and  $\text{Ta}_{25}\text{Nb}_{25}\text{W}_{25}\text{Mo}_{25}$  alloys [91]



alleviating the grain boundary brittleness and changing the fracture morphology from intergranular fracture to transgranular fracture. Consequently, both large plasticities of  $>10\%$ , along with high strength of  $>1750$  MPa at room temperature, are successfully achieved (Fig. 11).

In addition, some BCC HEAs also display certain tensile plasticity behavior, such as the TaNbHfZrTi HEA and its derivative [28]. J. Cízek et al. [92] reported that the HfNbTaTiZr exhibits a tensile yield strength of 1000 MPa, an ultimate strength of 1010 MPa and a total elongation to failure of 13% (Fig. 12).

In addition, heat treatment processing also has an influence on the mechanical property of alloys. Senkov et al. [93] examined the tensile properties of the TaNbHfZrTi HEA after being cold-rolled and then annealed at 1073 and 1273 K, respectively. As shown in Fig. 13, the 86.4% cold-rolled sheet had true tensile stress of 1295 MPa

**Fig. 11** Stress–strain curves of the as-cast base RHEA (black) and doped RHEAs with different contents of B at room temperature under compression [66]

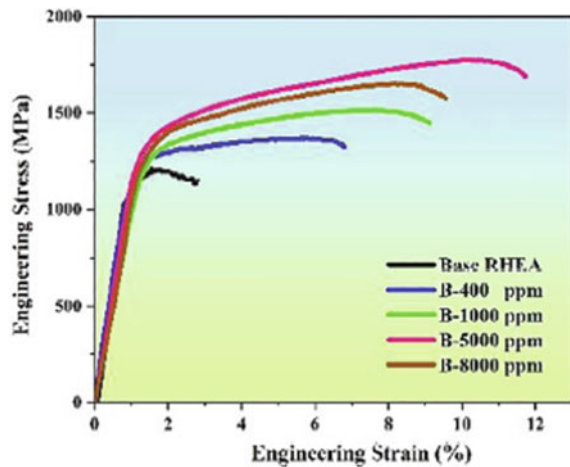
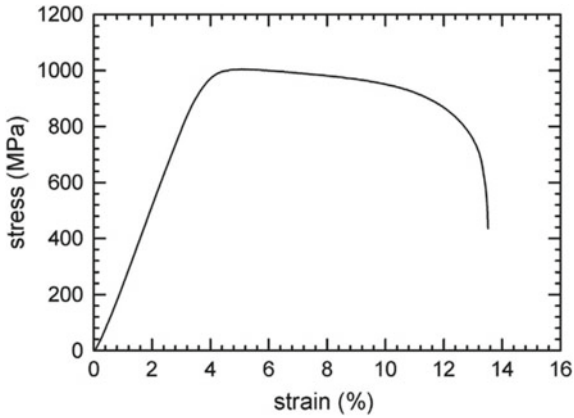




**Fig. 12** Stress–strain curve for tensile tests of standard size HfNbTaTiZr alloy in the as-cast state [93]



and tensile ductility of 4.7%. After annealing at 1000 °C, the true tensile stress and ductility of the sheet were 1262 MPa and 9.7%, respectively.

Wu et al. [94] reported a novel refractory HfNbTiZr HEA with a single BCC structure, which still holds the single BCC phase even after furnace cooling from homogenization at 1573 K for 6 h. The fracture strength and plastic strain of this HEA were about 969 MPa and 14.9%, respectively (Fig. 14). The significant work hardening behavior is considered as resulting from the movement and multiplication of dislocations. Then, Bu et al. [77] further confirmed that the observed local double cross-slips caused by the LCFs distribute dislocations onto various atomic planes homogenously, which is thought to be beneficial for ductility in HfNbTiZr HEAs.

Lei et al. [30] further reported that proper additions of oxygen e to NbHfZrTi could promote the formation of ordered nanoscale regions within the HEA characterized by (O, Zr, Ti)-rich atomic complexes. The ordered interstitial complexes change the

**Fig. 13** True stress–true strain curves of as-cold-rolled and rolled-and-annealed sheet of HfNbTaTiZr [8]

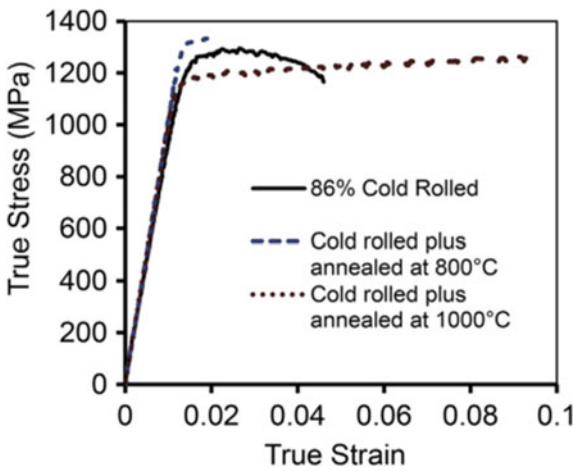
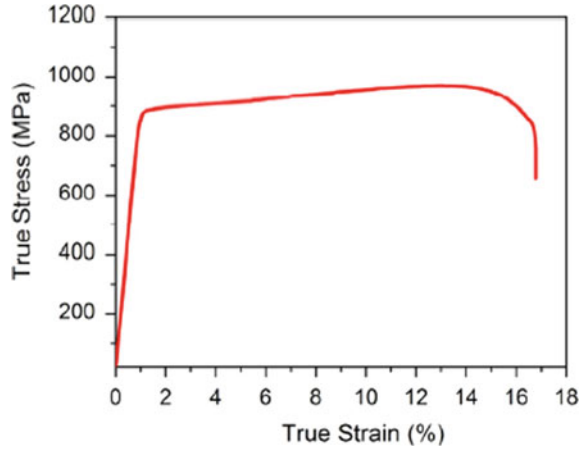


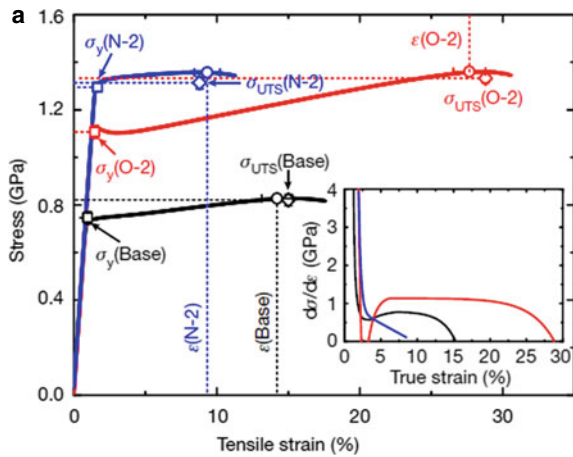
**Fig. 14** Tensile true stress–strain curve of HfNbTiZr alloy [95]



dislocation shear mode from planar slip to wavy slip and promote double cross-slip and thus dislocation multiplication through the formation of Frank–Read sources during deformation. Therefore, the yield strength increases from 0.75 GPa for the base HEA to 1.11 GPa for the doped O-2 HEAs, while the elongation has nearly doubled, increasing from 14.21% for the base HEA to 27.66% for the O-2 HEA, accompanied by a substantial work-hardening effect (Figs. 14 and 15).

Though BCC HEAs have recently attracted extensive attention for their excellent high-temperature mechanical property, the brittleness and low work-hardening rate at ambient temperature limit their practical uses. Serious efforts have been devoted, and a few solutions have been proposed [79, 95, 95]. Huang et al. [29] reported that via tailoring the stability of the constituent phases, transformation-induced ductility and work-hardening capability are successfully achieved in a brittle TaHfZrTi alloy.

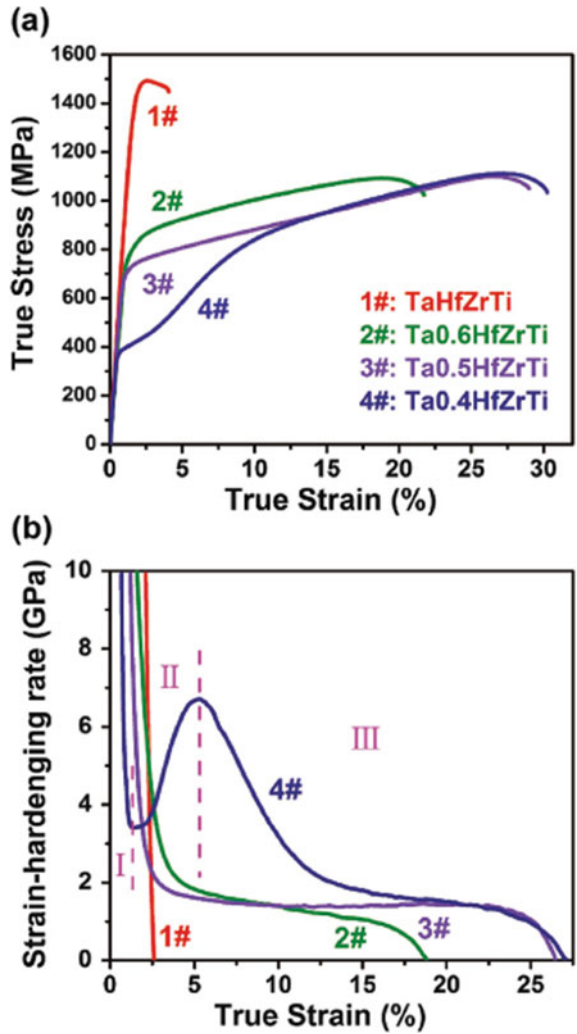
**Fig. 15** Room-temperature tensile stress–strain curves for the as-cast TiZrHfNb (denoted as base alloy), (TiZrHfNb)<sub>98</sub>O<sub>2</sub> (denoted as O-2) and (TiZrHfNb)<sub>98</sub>N<sub>2</sub> (denoted as N-2) HEAs. The inset shows the corresponding strain-hardening response [30]



Phase transformation yielded an intensive strain-hardening effect by dynamic strain–stress partitioning between the BCC and HCP phases and promote plastic deformation inside grains, which effectively suppressed early cracking and eventually gave rise to an outstanding combination of strength and ductility. As shown in Fig. 16, the plasticity of BCC HEAs was greatly improved from 4% (i.e., Ta1) to 27% (i.e., Ta0.4), although the fracture strength is slightly lowered to 1100 MPa with decreasing of Ta content.

Similarly, Wen et al. [80] further found that a proper addition of Nb to Ta0.2HfZrTi could not only enhance the TRIP effect due to the reduced phase stability of the prior BCC phase, but also facilitate twinning in the product HCP (hexagonal close packing)

**Fig. 16** Mechanical behavior of the as-cast  $Ta_x$  HEAs at room temperature. **a** Representative tensile true stress–strain curves. **b** The corresponding strain-hardening rate curves [29]



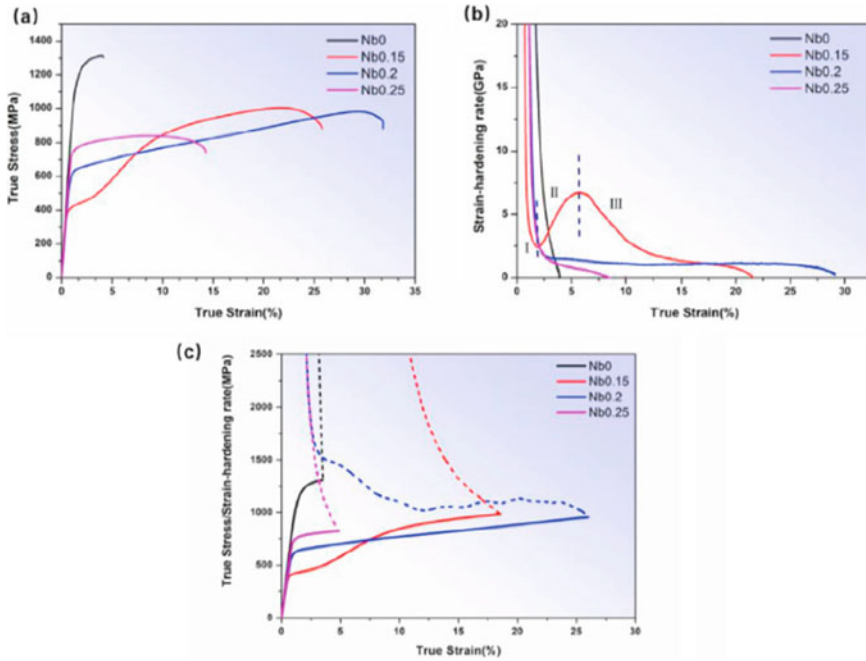


**Fig. 17** **a** Room-temperature tensile mechanical properties of the Nb<sub>x</sub> alloys, **b** the corresponding strain-hardening rate curves, and **c** curves of true stress/work-hardening rate against true strain [80]

phase at the late stage of deformation. As a result, the HfNb<sub>0.2</sub>Ta<sub>0.2</sub>TiZr HEA shows much enhanced mechanical properties, i.e., pronounced work-hardening behavior and large uniform ductility of up to 26% (Fig. 17).

### 3.2 Mechanical Behavior at Elevated Temperatures

BCC HEAs based on refractory elements have shown interesting properties at elevated temperatures, such as outstanding high-temperature strength, high oxidation, and corrosion resistance, which ensure them promising materials for high-temperature applications [44, 96]. Senkov et al. [14] found that at 600 °C and above, NbMoTaW and VNbMoTaW alloys showed extensive compressive plastic strain accompanied by the yield stress of both alloys dropped by 30–40% between room temperature and 600 °C and was relatively insensitive to temperature above 600 °C (Fig. 18). The high-temperature mechanical properties of these BCC HEAs compare favorably with conventional superalloys (Fig. 19).

Senkov et al. [96] researched the compression properties of a refractory TaNbHfZrTi alloy in the temperature range of 296–1473 K (Fig. 20) and found that the properties were correlated with the microstructure developed during compression

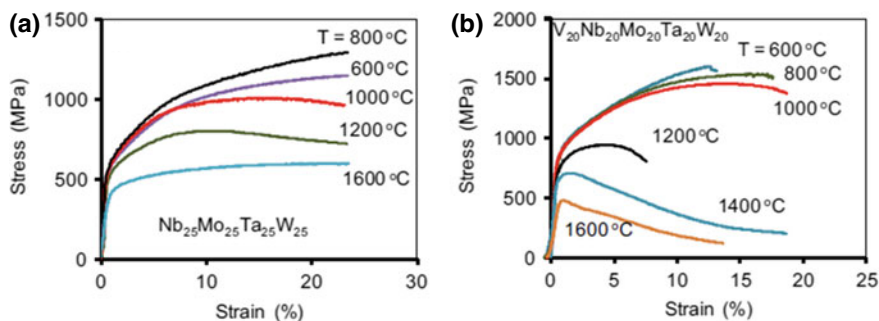


**Fig. 18** Compressive engineering stress–strain curve of the NbMoTaW and VNbMoTaW HEA at elevated temperatures [14]

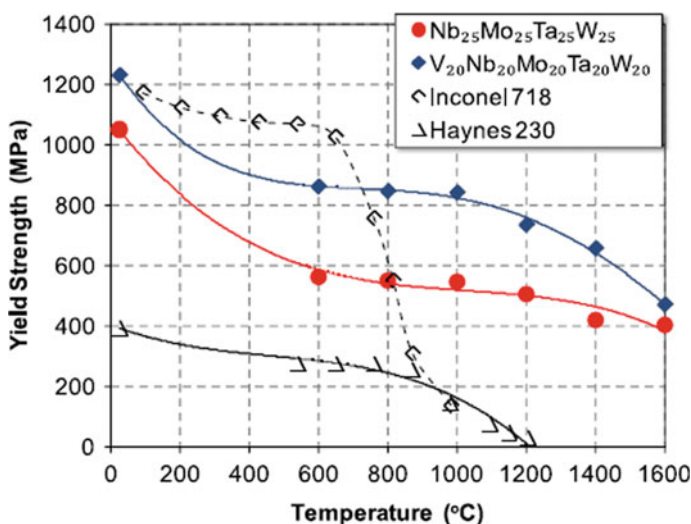
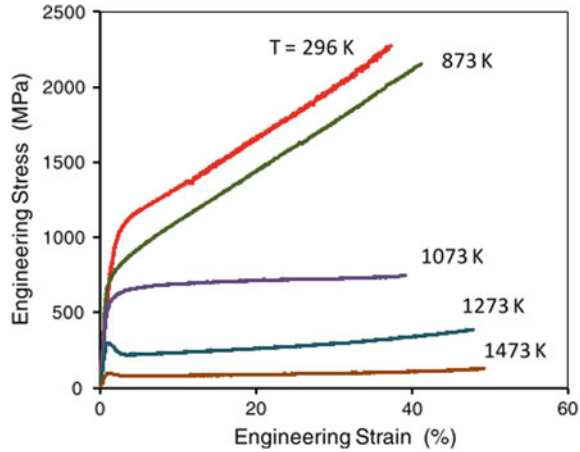


**Fig. 19** Temperature dependence of the yield stress of Nb<sub>25</sub>Mo<sub>25</sub>Ta<sub>25</sub>W<sub>25</sub> and V<sub>20</sub>Nb<sub>20</sub>Mo<sub>20</sub>Ta<sub>20</sub>W<sub>20</sub> HEAs and two superalloys [14]

testing. They reported the alloy had a yield strength of 929 MPa at 296 K, 790 MPa at 673 K, 675 MPa at 873 K, 535 MPa at 1073 K, 295 MPa at 1273 K and 92 MPa at 1473 K with a strain rate of  $10^{-3} \text{ s}^{-1}$  [96]. Continuous strain hardening and good ductility were observed in the temperature range from 296 to 873 K. Partial dynamic recrystallization, leading to the formation of fine equiaxed grains near grain boundaries, was observed in the specimens deformed at 1073, and 1273 K and completed dynamic recrystallization was observed at 1473 K.

Guo et al. [97] reported that at elevated temperatures, the MoNbHfZrTi alloy has a compression yield strength of 825 MPa at 1073 K, 728 MPa at 1173 K, 635 MPa

**Fig. 20** Engineering stress versus engineering strain compression curves of the TaNbHfZrTi alloy at different temperatures [96]



at 1273 K, 397 MPa at 1373 K, and 187 MPa at 1473 K, and some fine grains form at grain boundaries due to partial dynamic recrystallization (Fig. 21).

Feng et al. [98] used intrinsic material characteristics as the alloy-design principles to design CrMoNbV RHEA, which has high-temperature strengths (beyond 1000 MPa at 1273 K), superior to other reported RHEAs as well as conventional superalloys, as shown in Fig. 22. And the outstanding elevated-temperature mechanical properties were attributed to its large atomic-size and elastic-modulus mismatches, the insensitive temperature dependence of elastic constants, and the dominance of non-screw character dislocations caused by the strong solute pinning, thus leading to pronounced solid-solution strengthening effect.

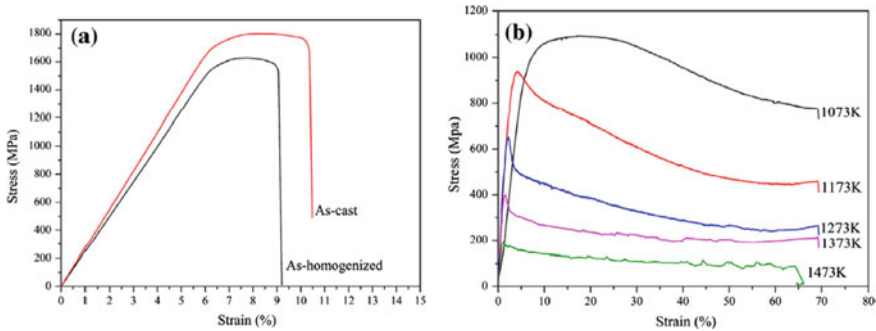


**Fig. 21** Compressive curves of MoNbHfZrTi alloy: **a** at room temperature and **b** at different elevated temperatures [97]